Phase diagram of the 3D quantum anisotropic XY model—A quantum Monte Carlo calculation

M. Guimarães [a,*], B.V. Costa [a], A.S.T. Pires [a], A. Souza [b]

[a] Departamento de Física, ICEX, UFMG, 30123-970, Belo Horizonte, MG, Brazil
[b] Departamento de Física, Universidade Rural Federal de Pernambuco, Recife, Pernambuco, Brazil

ABSTRACT

In this work we apply the stochastic series expansion quantum Monte Carlo method to study the quantum phase transition of the spin 1 three-dimensional XY model with easy-plane anisotropy D. We simulate this model in cubic lattices ($L \times L \times L$) with $L \in (4,24)$ and periodic boundary condition. Using finite size scaling we obtained the phase diagram for the model, the critical exponent $zv = 0.501(5)$ and the quantum critical point $D_c = 9.7950(3)J$. Using a low temperature expansion for the magnetic susceptibility we obtained $zv = 0.59(1)$.

© 2012 Elsevier B.V. All rights reserved.

1. Introduction

Classic order–disorder transitions are characterized as a change in the balance between the ordering arising from minimizing energy and the disordering arising from maximizing entropy, both driven by the temperature of the system. The expression quantum phase transition (QPT) is widely used when a transition takes place at temperature $T=0$, i.e., at any point of non-analyticity of the ground state energy of the system under investigation [1,2]. Classical transitions are driven by thermal fluctuations while QPT are driven by quantum fluctuations at $T=0$ as a parameter of the Hamiltonian, let us call it D, is tuned to disorder the ground state of the system at the critical point D_c. In general the physics behind a QPT is quite complex. The quantum critical point (QCP) can appear at an isolated point in a $T \times D$ diagram or at the end point of a continuous classical transition line [1]. At the QCP, quantum fluctuations exist on all length scales, therefore it can be seen at the vicinity of D_c for $T \approx 0$.

Many techniques like Quantum Monte Carlo, Exact Diagonalization, the self-consistent harmonic approximation (SCHA) and the bond operator formalism can be used to search the QCP. In this paper we use a Quantum Monte Carlo technique to study the three-dimensional anisotropic XY model of localized quantum spins described by the Hamiltonian

$$\mathcal{H} = \sum_{\langle i,m \rangle} J_k S_i^x S_m^x + S_i^y S_m^y + \sum_i D(S_i^z)^2, \qquad (1)$$

where $\langle i,m \rangle$ stands for a nearest neighbor pair of $S=1$ spins and $k=1$, 2 label inter-plane and intra-plane exchange interactions respectively. D is the single ion anisotropy. In Fig. 1 it is shown a *croquis* of the arrangements used in this work.

The present study is restricted to the case of antiferromagnetic interactions ($J_1 J_2 > 0$), with easy plane anisotropy ($D > 0$). For $D > D_c$ the system is in a disordered, gapped phase (massive), characterized by the total magnetization $M_{total}^z = \sum_i S_i^z = 0$. The region $D < D_c$ is gapless (massless) and the system is in an ordered phase. When the system approaches D_c on the $T=0$ line it undergoes a pure QPT. The correlation time diverges: $\tau_c \propto \xi^z$, where ξ is the correlation length and z is the dynamical critical exponent. This model has been studied by Pires and Costa [3] using the SCHA and the bond operator formalism in the small and large D phases respectively. The authors obtained the entire $T_c \times D$ critical diagram using SCHA formalism. It was found that as D approaches D_c from above the energy gap vanishes continuously as $\Delta \propto (D-D_c)^B$. They obtained: $B=1$ for $\alpha = J_2/J_1 = 0$, $B=0.6$ for $0 < \alpha < 1$, $B=0.5$ for $\alpha = 1$ and $B=0$ for $J_2/J_1 = 0$. The value $B=0.5$ is in agreement with the work of Wang and Wang [4]. An expression for the gap as a function of temperature was obtained as $m^2 = c_0 + c_1 T^{3/2} e^{-c_2/T}$ [3] where c_0, c_1 and c_2 are constants that depend on D and J_2/J_1. The phase diagram obtained by Pires and Costa is pictured in Fig. 2 in a plot $T_c \times D$ as a solid line. An interesting result obtained was a slight increase in T_c with increasing D for small D. A more pronounced effect was observed by Wang and Wang [4] and by Wang and Wong [5] using the bond operator and the series expansion method respectively. This effect can also be seen in the Heiseberg model [4–6]. As it is well known, the SCHA is a reasonable semi-classical approximation to calculate the transition temperature and low-temperature
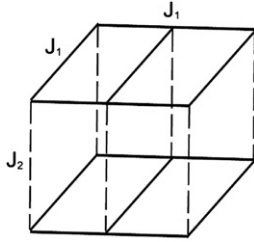
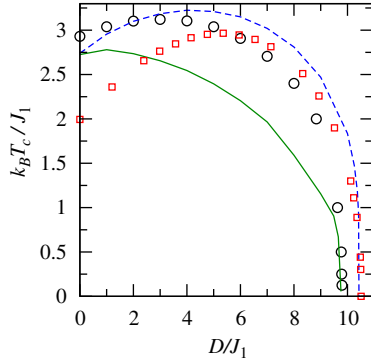**Fig. 1.** Croquis of the interaction arrangements used in this work.

Fig. 2. Phase diagram, T_c as a function of D for $J_2/J_1 = \alpha = 1.0$. The solid line is the result obtained by Pires and Costa [3] using the self-consistent harmonic approximation. The squares represent the results of Wang and Wang [4] using the bond operator approximation. The circles are the results of the present work using QMC. As a matter of comparison we plot the results of Pan [6] for the isotropic Heisenberg model as a dashed line.

($T < T_c$) properties of a system, however it is of limited value in estimating critical properties [7–10]. The bond operator is best suited to the large D phase, provided that the transition occurs at a relatively large D [3]. Nevertheless, a control of the calculations based on such approaches is very difficult. Only rigorous analytical results or numerical simulations can estimate the regime of validity of these methods. In this work we employ the QMC method to obtain the phase diagram of the model and the critical exponents B and v. We compare our results with the analytical calculations available from previous works as shown in Fig. 2. We found that SCHA and the Bond operator reproduce the phase diagram reasonable well. The fact that the SCHA gives better results than the bond operator approach in the entire phase space when compared with our results is noteworthy. We also develop an approach in order to judiciously obtain the critical exponent v.

2. Quantum Monte Carlo—results

In our Quantum Monte Carlo (QMC) simulations of the Hamiltonian 1 we use the code developed by the ALPS group [11] which is based on the Stochastic Series Expansion (SSE) [12] and use the directed loop update scheme developed by Sandvik [13] implemented with an optimal-local stochastic matrix for the algorithm [14]. The SSE approach is based on the high temperature expansion of the partition function up to order M, being a generalization of Handscomb' algorithm [15] used to study the ferromagnetic Heisenberg model. The SSE method does not bear from usual convergence difficulties found in the Suzuki–Trotter formulation [16,17].

Thermodynamical quantities, such as the total energy $\langle E \rangle$, susceptibility $\langle \chi \rangle$ and spin stiffness $\langle \rho \rangle$ are straightforwardly obtained as derivatives of the free energy. The spin stiffness in particular can be defined as the increase in the free energy due to

imposing a twist in the boundary condition on the order parameter [18]. In the simulation the spin stiffness is given by the "winding numbers", i.e., the net spin current across the periodic boundaries in the directions x and y (for simulations performed in the z quantization axis). In analogy with the superfluid density of a boson system [19,20] one can demonstrate that [21]

$$\rho = \left.\frac{\partial^2 E(\theta)}{\partial \theta^2}\right|_{\theta=0} = \frac{\langle W_x^2 \rangle + \langle W_y^2 \rangle}{2N\beta}, \qquad (2)$$

where $E(\theta)$ is the internal energy per spin, β is the inverse temperature and W_x and W_y are the winding numbers.

To build the phase diagram we use the finite size scaling behavior of the thermodynamic functions. We have simulated systems of size ($L \times L \times L$) with periodic boundary conditions. For parameters $D < 0.9D_c$ we used 20 000 Monte Carlo Steps (MCSs) for thermalization for even lattice sizes $L \in [4,16]$. For $D \approx D_c$ we used 50 000 MCS for even lattice sizes $L \in [4,24]$. In both cases the number of configurations used for measurements was 10 times the number of MCS used for thermalization. For $D > D_c$ we used 100 000 MCS for thermalization for even lattice sizes $L \in [4,10]$ and around 5 000 000 MCS for measurements. Throughout this work the error bars are not shown in figures, only if they are smaller than the symbols. At the critical temperature, T_c, the spin stiffness has a fixed point that scales as $\rho \approx L^{2-d}P_\rho(|(T_c-T)/T_c|L^{1/v})$ [18], where L is the linear lattice size. Ploting ρL as a function of T we expect that all curves intercept at a fixed point $\rho(T_c)L = const.$ The critical temperature is obtained assuming the scaling, $T_c \approx T_c(\infty) + AL^{-1} + O(L^{-2})$, holds for $D < D_c$. Slightly above the $T \approx 0$ line we notice a continuous drop of the spin stiffness order parameter as the anisotropy is increased from $D < D_c$ to $D > D_c$.

For $D < D_c$, if we plot $\rho(L,t)L/T$ as a function of $|t|L^{1/v}$ we can choose v such that the results for several values of L collapse into the same curve. This procedure gives an estimate of the critical index v. In Fig. 3 it is shown the typical behavior of the spin stiffness for $D = 0$ and $\alpha \equiv J_2/J_1 = 1$. The estimate obtained for the critical temperature and the critical exponent is $k_b T = 2.93J$ and $v = 0.66$ respectively. The value of T_c is quite close to the one obtained by the use of the SCHA approach even though far from the bond operator result (see Fig. 2).

As observed in previous works [3–6] we can confirm an increase in T_c with increasing D, for small D as seen in Fig. 2. One could argue that the increase of D from 0 slightly changes the behavior of the system from XY to planar rotator, which has a higher transition temperature. As D is increased further quantum fluctuations reduces the magnetic order, thus reducing the transition temperature until it reaches the critical value D_c at $T = 0$.
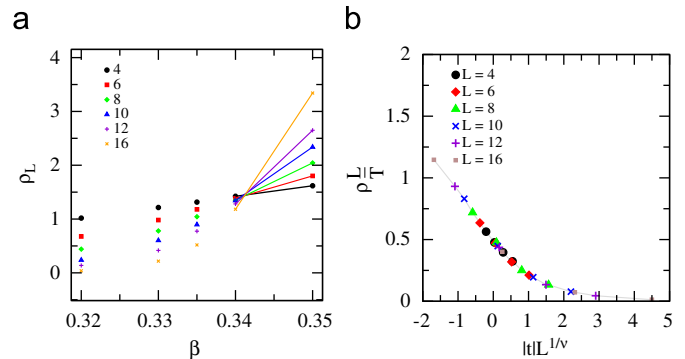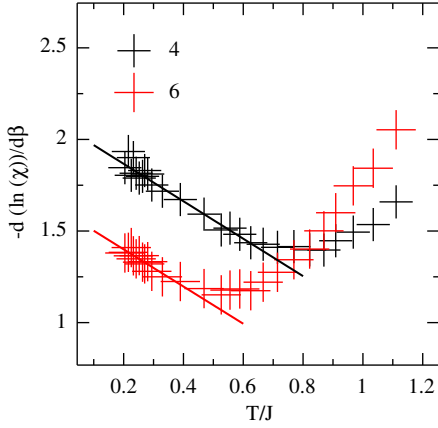

Fig. 3. Figs. a, b show the finite size scaling stiffness analysis of the spin stiffness for $D = 0$ and $\alpha = 1$. Fig. (a) shows the fixed point for $L\rho(T_c)$. In Fig. (b) is shown the collapse of the curves for several values of L. From an analysis of these figures we obtain $k_b T_c = 2.93J$ and $v = 0.66$.

Fig. 4. Evaluation of the exponent n of Eq. (3) using the derivative of the logarithm of susceptibility for lattice size 4 (top); $n = 1.02 \pm 0.08$ and 6 (bottom) $n = 1.0 \pm 0.1$ for anisotropy $D = 10.1$.
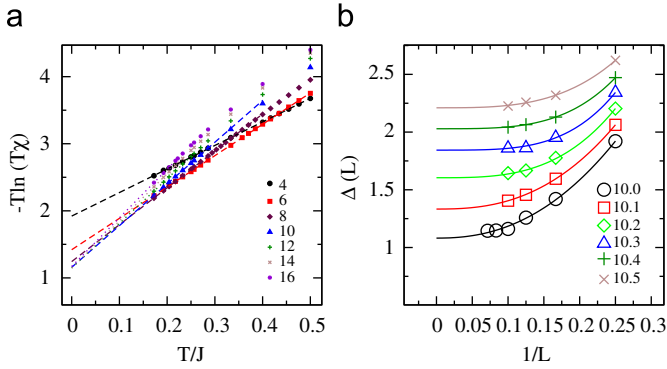
Fig. 5. (a) Finite size gap obtained for several lattice sizes as the intercept of plot $T \ln(T\chi_\infty)$ by T at anisotropy $D = 10.0$. (b) Finite size scaling of the gap for several anisotropies $D > D_c$ according to Eq. (4).

Fig. 6. The Figs. (a) and (b) show a log-log plot of the gap as a function of the relative anisotropy ($t = D - D_c$) for $\alpha = 1.0$ and 0.5 respectively. Two different sets of anisotropies (circles and squares) were used to estimate the error of zv for $\alpha = 1.0$. The slope of the curves provides $zv = 0.59(1)$ for $\alpha = 1.0$ with $D_c = 9.795$ and $0.62(3)$ for $\alpha = 0.5$ with $D_c = 8.03$.
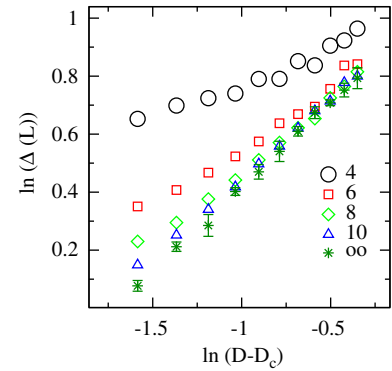
Fig. 7. The figure show log–log plot of finite size gap as a function of the relative anisotropy ($t = D - D_c$) for $\alpha = 1.0$ with $D_c = 9.795$. The slope of the curve provides zv (0.24, 0.41, 0.48, 0.54, 0.59) for simulated lattices 4, 6, 8, 10 and the infinity size extrapolated gap represented by the star.

Beyond the critical anisotropy $D > D_c$, we assume a low temperature expansion for the magnetic susceptibility based on an expression derived by Troyer [22]
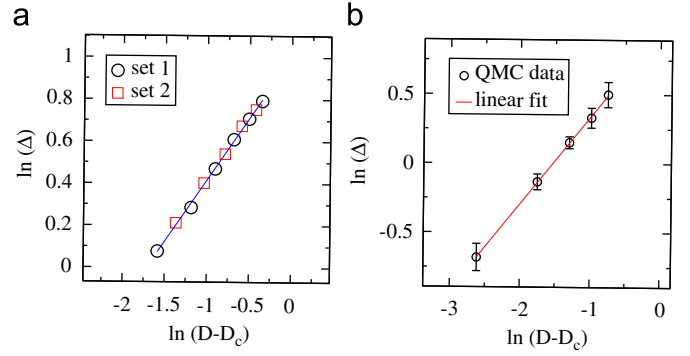
$$\chi(L) \approx \beta^{-n} \exp(-\beta\Delta(L)), \qquad (3)$$

where $\Delta(L)$ is the gap for the finite size lattice and β is the inverse temperature. The parameter n depends on the shape of the dispersion relation. The derivative of the logarithm of the susceptibility $-\partial \ln(\chi(L)/\partial\beta$ provides a way to estimate the parameter n. At low temperature this derivative is $\Delta(L) + nT$. The slope n is close to -1 for small systems sizes (4, 6) (see Fig. 4). In a very naive approach we can estimate the gap by supposing that $\Delta(L) \approx \Delta(\infty) + AL^m$. Solving the equation of $\chi(L)$ for $\Delta(L)$ and substituting in the previous equation with $n = -1$ we obtain

$$\Delta(L) = -T \ln(T\chi(L)) = \Delta\infty + AL^m. \qquad (4)$$

Logarithmic corrections, if present, require simulations of much larger lattice sizes than the ones performed in the present work. In Fig. 5(a) we show a plot of $-T \ln(T\chi)$ as a function of the inverse temperature for several lattice sizes. By adjusting a straight line to the data, an estimate of the finite size gap is given by the intercept of the curve. In Fig. 5(b) we show a plot of $\Delta(L)$ as a function of inverse lattice size for several anisotropies. By adjusting a curve to the data, according to Eq. (4), an estimate of the infinite size gap is obtained.

In Figs. 6 and 7 it is shown a plot of $\ln \Delta$ as a function of $D - D_c$ obtained by this approach. The slope of the curves provides an estimate for $B = zv$ [1].

As the anisotropy approaches the critical value D_c the quantum fluctuations become stronger in such a way that the finite size scaling for the spin stiffness has to be modified to [23]

$$\rho(L, t, T) = \frac{1}{L^{d-2}L_\tau} F_\rho(L^z T, tL^{1/v}), \qquad (5)$$

where $F_\rho(TL^z, tL^{1/v})$ is a homogeneous function of its arguments, $t = 1 - D/D_c$ and $\xi_\tau \to L_\tau \propto 1/T$.

Similarly, the modified finite size scaling for the uniform magnetic susceptibility is given by [23]

$$\chi(L, t, T) = \frac{L_\tau}{L^d} F_\chi(L^z T, tL^{1/v}), \qquad (6)$$

Using Eq. (5) we can sweep z and D_c until a good collapse in a plot of $\rho(L, t)L^{d-2}/T$ by TL^z is found. In Fig. 8 it can be seen the best collapses for $\alpha = 1.0$ and $\alpha = 0.5$ with $D_c = 9.8$, $z = 0.9$ and $D_c = 8.0$, $z = 0.6$ respectively. A value of $z < 1$ is obviously not the correct asymptotic behavior, and upon going to larger systems we believe that z would increase to 1. A collapse can be seen in Fig. 9 for the susceptibility assuming $z = 1$.

If the temperature is low enough Eq. (5) can be used ignoring the first argument in the scaling function [24]. A plot of ρL^2 by $|tL^{1/v}|$ should produce the intended collapse as shown in Figs. 10 and 11 for $\alpha = 1.0$ and $\alpha = 0.5$ respectively. As usually seen in the path integral formulation, the mapping of the quantum to a classical corresponding system relates temperature with a imaginary time dimension $L_\tau \propto 1/T$ [25]. Since time and space are not equivalent, we have two correlation "lengths", a spatial ξ and a
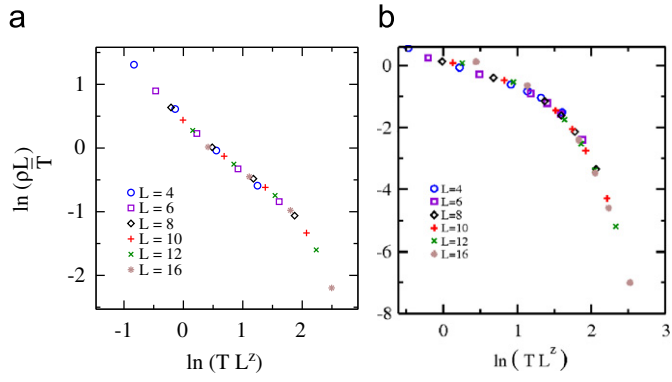
Fig. 8. Finite size scaling stiffness analysis of the spin stiffness in a log–log plot of $\rho(L,t)L^{d-2}/T$ by TL^z. It is shown the collapse of the stiffness curves for several values of L. In Fig. (a) a good stiffness collapse was found with $D=9.8$ and $z=0.9$ for $\alpha=1.0$. In Fig. (b) a good stiffness collapse was found with $D=8.0$ and $z=0.66$ for $\alpha=0.5$.
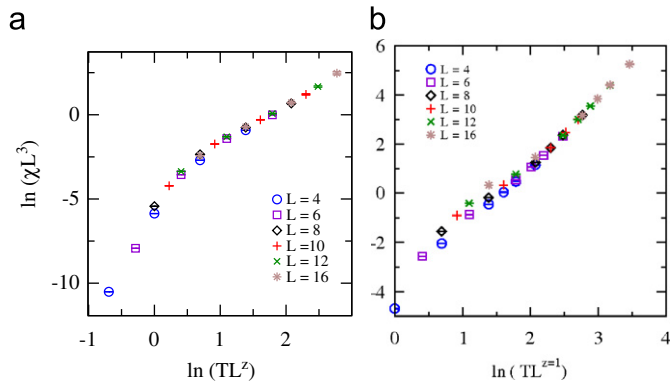
Fig. 9. Finite size scaling collapse of susceptibility according to scaling hypothesis of Eq. (6) assuming $z=1$ with (a) $D_c=9.8$ for $\alpha=1.0$, (b) $D_c=8.0$ for $\alpha=0.5$.
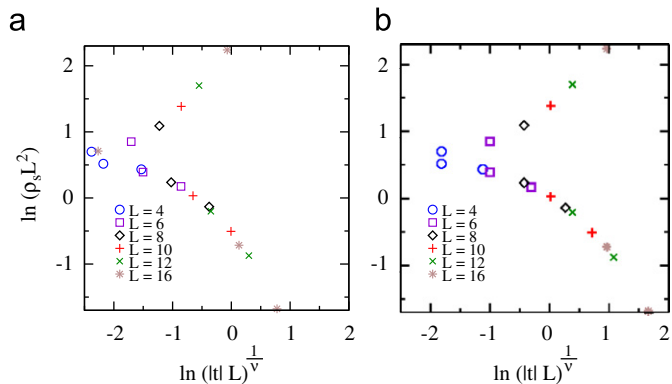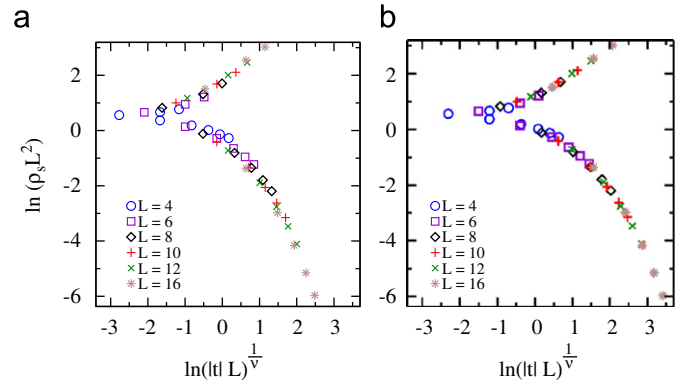

Fig. 10. Finite size scaling collapse of spin stiffness according to scaling hypothesis of Eq. (7) at $k_bT=0.125J$ for $\alpha=1.0$. It was found reasonable collapses for a wide range of parameters. (a) $\nu=0.6$, $D_c=9.79$; (b) $\nu=0.5$, $D_c=9.80$.

temporal ξ_τ correlation. These are connected by the dynamical critical exponent $z: \xi_\tau \propto \xi^z$.

If a fixed aspect ratio between the imaginary time (inverse temperature) and space is set as $const = L^z/L_\tau \propto TL^z$ then Eq. (5) reduces to

$$\rho(L,t)L^{d+z-2} = F_\rho(const, tL^{1/\nu}). \tag{7}$$

At the critical anisotropy ($t=0$) curves for different lattice sizes should cross each other. In Fig. 12 it can be noticed that three data

Fig. 11. Finite size scaling collapse of spin stiffness according to scaling hypothesis of Eq. (7) at $k_bT=0.25J$ for $\alpha=0.5$. We found reasonable collapses for a wide range of ν with $D_c=8.05$. (a) $\nu=0.6$, (b) $\nu=0.5$.
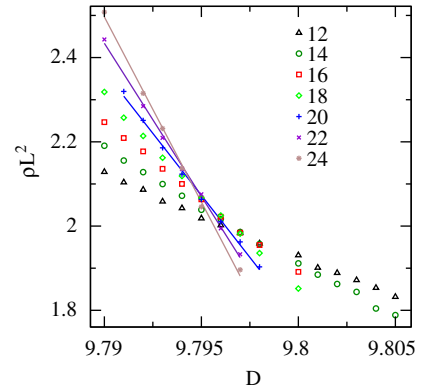
Fig. 12. Finite size scaling of the spin stiffness according to Eq. (7). The crossing points tends towards the critical coupling D_c.

points with highest lattice sizes cross each other close to the same point assuming $z=1$. Each of these three crossing points give an estimate for the critical anisotropy. Repeating this calculation for four different simulations we obtain $D_c = 9.7945(5)$.

A precise estimative of D_c and ν can usually be achieved by collapsing the stiffness data for different L using a correction to Eq. (7). The usual ansatz is the choice $N(L) = 1 + cL^{-w}$ [24,26].

The corrected stiffness scaling relation is given by

$$\rho(L,t)L^{d+z-2} = N(L)F_\rho(const, tL^{1/\nu}). \tag{8}$$

The $N(L)$ normalization factor is introduced to take into account subleading corrections to scaling. Any attempt to adjust our results with this ansatz or other ansatz [27] were fruitless, generating large error bars to the exponents. For example, the exponent ν adjusts well for any value in the interval 0.5 and 0.6 for D_c close to 9.78 and 9.80 for a wide range of values of w. The leading term itself was difficult to determine accurately, which can be seen in Fig. 13 where noticeably different values of ν still produce fine collapses.

The main concern at this point is the way the $N(L)$ dependence can be removed. Suppose that the scaling function F_ρ in Eq. (8) admits a series of expansion in $t = 1 - D/D_c \approx 0$

$$\rho(L,t)L^{d+z-2} = N(L)(F_\rho(0) + F'_\rho(0)tL^{1/\nu} + O(t^2)), \tag{9}$$

$$\rho(L,t)L^{d+z-2} \approx A(L) + B(L)t. \tag{10}$$

By performing a linear fit to $\rho(L,t)L^{d+z-2}$ it is then possible to obtain the independent term $A(L) = N(L)F_\rho(0) \approx \rho(L,0)L^{d+z-2}$. The $N(L)$ dependence is then eliminated by dividing $\rho(L,t)L^{d+z-2}$
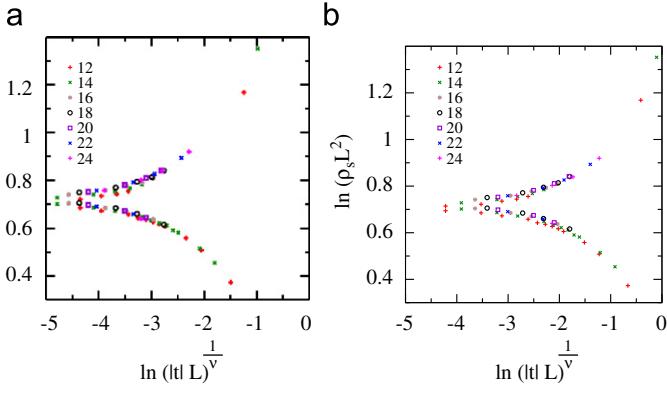
Fig. 13. The figure shows the finite size scaling collapse of stiffness according to scaling hypothesis in Eq. (7) with $T \propto 1/L$ for $\alpha = 1.0$. It was found reasonable collapses for a wide range of v with $D_c = 9.795$. (a) $v = 0.6$, (b) $v = 0.5$.
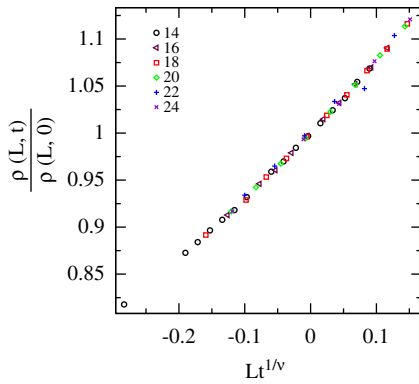
Fig. 14. The collapse of spin stiffness curves is shown for several lattice sizes obtained by the value $v = 0.501(5)$ and $D_c = 9.7948(3)$ which produced the least average error of v evaluated from Eq. (14). The error bars were calculated according to the second procedure described in the text.

by $A(L)$

$$\frac{\rho(L,t)L^{d+z-2}}{A(L)} \approx 1 + \frac{F'_\rho(0)}{F_\rho(0)} tL^{1/v} \approx \frac{\rho(L,t)}{\rho(L,0)}. \tag{11}$$

Therefore, if we plot of $\rho(L,t)/\rho(L,0)$ as a function of $tL^{1/v}$ with an appropriate value for v and D_c, curves for different values of L will collapse into the same curve. The result is shown in Fig. 14.

The error bars involved in the collapse procedure were calculated using two different methods. The first one is done by taking the average residue of a third order polynomial fit to the stiffness simulation data of the highest lattice sizes (12, 14, 16, 18, 20, 22, 24). The estimate of D_c and v is given by the values that produce the smallest average residue. The final result is given by the average value obtained from four independent simulations. This procedure yields the following result: $D_c \in [9.7912, 9.7923]$, and $v \in [0.485, 0.492]$. Performing a similar calculation with the uniform magnetic susceptibility we obtain $D_c \in [9.7870, 9.7910]$ and $v \in [0.505, 0.523]$. The second method for estimating the error bars depends on the error involved in the estimate of v. Observing Eq. (10) we can expect that the slope of ρL^{d+z-2} has the following L dependence:

$$\frac{\partial \rho(L,t)}{\partial t}\bigg|_{t=0} L^{d+z-2} \approx N(L)L^{1/v}. \tag{12}$$

We can take its logarithm to find

$$(d+z-2)\ln(L) + \ln\left(\frac{\partial \rho(L,t)}{\partial t}\bigg|_{t=0}\right) \approx \ln(N(L)) + \ln(L)\frac{1}{v}. \tag{13}$$
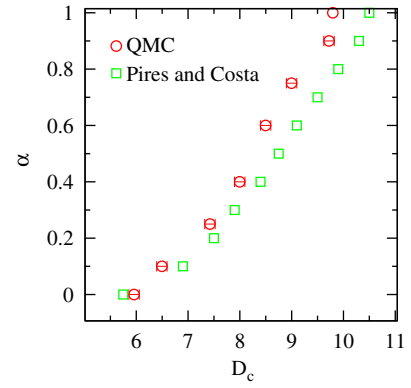
Fig. 15. This figure shows the behavior of critical anisotropy as a function of the parameter $\alpha = J_2/J_1$. The squares are the bond operator results of Pires and Costa, the circles are from the present work and were obtained using scaling according to Eq. (7).

Subtracting the previous equation for different lattice sizes L and L', we obtain

$$(d+z-2)\left(\ln\left(\frac{L}{L'}\right) + \ln\left(\frac{\frac{\partial \rho(L,t)}{\partial t}\big|_{t=0}}{\frac{\partial \rho(L',t)}{\partial t}\big|_{t=0}}\right)\right)$$
$$\approx \ln\left(\frac{N(L)}{N(L')}\right) + \ln\left(\frac{L}{L'}\right)\frac{1}{v}.$$

Isolating v and assuming $\ln(N(L)) - \ln(N(L')) \approx 0$ and $z = 1$ we obtain a way to estimate v similar to Ref. [28]

$$v = \frac{\ln(L) - \ln(L')}{\ln\left(L^2 \frac{\partial \rho(L,t)}{\partial t}\big|_0\right) - \ln\left(L'^2 \frac{\partial \rho(L',t)}{\partial t}\big|_0\right)}. \tag{14}$$

The best collapse is then defined by the values v and D_C which produce the minimum average deviation of v obtained using a set of couple (L, L') from the highest simulated lattice sizes (12, 14, 16, 18, 20, 22, 24). Again the final result is given by the average value of four independent simulations. Using this criterion we obtained $D_c \in [9.7943, 9.7951]$, and $v \in [0.496, 0.505]$ from spin stiffness and $D_c \in [9.7935, 9.7946]$, and $v \in [0.47, 0.51]$ from susceptibility.

The final estimate is given by

$$D_c = 9.7948(3) \quad v = 0.501(5),$$
$$D_c = 9.7941(5) \quad v = 0.49(2),$$

using stiffness and susceptibility respectively.

The critical anisotropy $D_c(\alpha)$ shown in Fig. 15 can be obtained by the crossing point of ρL^2 by D according to Eq. (7) for two different lattice sizes (14, 16). The statistical errors are smaller than systematic error due to finite size. Therefore, the error bars were estimated by the difference from the crossing from the lowest (4, 6) to the highest (14, 16) crossing points.

3. Conclusion

In this work we have studied the quantum phase transition in the three dimensional anisotropic XY model using a Monte Carlo numerical calculation. We found that contrary to the expected the SCHA works quite well in the whole range of anisotropy. The bond operator method that should work in the large D region does not give good results when compared to the SCHA. One possible explanation is that the SCHA works well for low temperatures and renormalizations of the harmonic interactions considered by Pires and Costa took into account thermal and quantum fluctuations while the bond operator results relied on a mean field value for

the t bosons and the global chemical potential. To obtain the critical exponent v we have proposed a finite size scaling that seems to work very well in the present case.

References

[1] S. Sachdev, B. Keimer, Quantum criticality, 2011, arXiv:1102.4628v2.
[2] Mucio A. Continentino, Quantum Scaling in Many-Body Systems, World Scientific, Singapore, River Edge, NJ, 2001. ⟨http://www.worldscientific.com/doi/abs/10.1142/9789812798909_0001⟩.
[3] A. Pires, B. Costa, Physica A: Statistical Mechanics and its Applications 388 (2009) 3779.
[4] H.-T. Wang, Y. Wang, Physical Review B 71 (March) (2005) 104429 http://link.aps.org/doi/10.1103/PhysRevB.71.104429.
[5] W.H. Wong, C.F. Lo, Y.L. Wang, Physical Review B 50 (September) (1994) 6126 http://link.aps.org/doi/10.1103/PhysRevB.50.6126.
[6] K.-K. Pan, Physics Letters A 374 (2010) 3225.
[7] J. Villain, Journal de Physique France 35 (1974) 27 http://dx.doi.org/10.1051/jphys:0197400350102700.
[8] J. Villain, Journal de Physique 36 (1975) 581, ISSN 0302-0738, http://dx.doi.org/10.1051/jphys:01975003606058100.
[9] S. Leonel, A.C. Oliveira, B. Costa, P.Z. Coura, Journal of Magnetism and Magnetic Materials 305 (2006) 157. ISSN ISSN 0304-8853, ⟨http://www.sciencedirect.com/science/article/pii/S0304885305011662⟩.
[10] S.A. Leonel, A.S.T. Pires, Brazilian Journal of Physics 30 (06) (2000) 428, ISSN 0103-9733.
[11] A. Albuquerque, F. Alet, M. Troyer, et al., Journal of Magnetism and Magnetic Materials 310 (2007) 1187, ISSN 0304-8853, Proceedings of the 17th International Conference on Magnetism, The International Conference on Magnetism, 0801.1765v1.
[12] O.F. Syljuåsen, A.W. Sandvik, Physical Review E 66 (October) (2002) 046701 http://link.aps.org/doi/10.1103/PhysRevE.66.046701.
[13] F. Alet, S. Wessel, M. Troyer, Physical Review E 71 (March) (2005) 036706 http://link.aps.org/doi/10.1103/PhysRevE.71.036706.
[14] L. Pollet, S.M.A. Rombouts, K. Van Houcke, K. Heyde, Physical Review E 70 (November) (2004) 056705 http://link.aps.org/doi/10.1103/PhysRevE.70.056705.
[15] D. Handscomb, Proceedings of the Cambridge Philosophical Society 58 (1962) 594.
[16] M. Suzuki, Progress of Theoretical Physics 56 (1976) 1454.
[17] H.F. Trotter, Proceedings of the American Mathematical Society 10 (1959) 545.
[18] M.E. Fisher, M.N. Barber, D. Jasnow, Physical Review A 8 (August) (1973) 1111 http://link.aps.org/doi/10.1103/PhysRevA.8.1111.
[19] E.L. Pollock, D.M. Ceperley, Physical Review B 36 (December) (1987) 8343 http://link.aps.org/doi/10.1103/PhysRevB.36.8343.
[20] M.P.A. Fisher, P.B. Weichman, G. Grinstein, D.S. Fisher, Physical Review B 40 (July) (1989) 546 http://link.aps.org/doi/10.1103/PhysRevB.40.546.
[21] A.W. Sandvik, Physical Review B 56 (November) (1997) 11678 http://link.aps.org/doi/10.1103/PhysRevB.56.11678.
[22] M. Troyer, H. Tsunetsugu, D. Würtz, Physical Review B 50 (November) (1994) 13515 http://link.aps.org/doi/10.1103/PhysRevB.50.13515.
[23] A.V. Chubukov, S. Sachdev, J. Ye, Physical Review B 49 (May) (1994) 11919 http://link.aps.org/doi/10.1103/PhysRevB.49.11919.
[24] A.W. Sandvik, AIP Conference Proceedings 135 (2010) 1297 arXiv:1101.3281v1 http://dx.doi.org/10.1063/1.3518900.
[25] S.L. Sondhi, S.M. Girvin, J.P. Carini, D. Shahar, Reviews of Modern Physics 69 (January) (1997) 315 http://link.aps.org/doi/10.1103/RevModPhys.69.315.
[26] L. Wang, K.S.D. Beach, A.W. Sandvik, Physical Review B 73 (January) (2006) 014431 http://link.aps.org/doi/10.1103/PhysRevB.73.014431.
[27] K.B. Ling Wang, A.W. Sandvik, arXiv(2005), mat0505194v1.
[28] M.H. Aloysius, P. Gottlob, Physica A: Statistical Mechanics and its Applications 201 (1993) 593. ISSN 0378-4371, ⟨http://www.sciencedirect.com/science/article/pii/037843719390131M⟩.